S_N2 reactions at amide nitrogen – theoretical models for reactions of mutagenic *N*-acyloxy-*N*-alkoxyamides with bionucleophiles

Stephen A. Glover

Division of Chemistry, School of Biological, Biomedical and Molecular Sciences, University of New England, Armidale, New South Wales 2351, Australia
E-mail: sglover@metz.une.edu.au

Dedicated to Oswald S. Tee on the occasion of his 60th birthday, and in recognition of his many contributions to chemistry in Canada

(received 09 Sep 01; accepted 21 Jan 02; published on the web 29 Jan 02)

Abstract

The reactions of *N*-formyloxy-*N*-methoxyformamide **4** with ammonia **2** and methanethiol **3** have been modeled at theAM1, HF/6-31G* and Density Functional computational levels. The reaction process is similar geometrically and electronically to classical S_N2 reactions at carbon. Near-linear transition states reveal extensive charge separation and partial nitrenium ion character at the formamide nitrogen indicative of a non-synchronous process involving early stretching of the formate-formamide nitrogen bond. Activation energies, computed from pBP/DN* energies of HF/6-31G* ground state and transition state geometries, are in the range of experimental values and a strong solvation effect is predicted. Evidence for anomeric weakening of the *N*-formate bond by the geminal alkoxyl oxygen was obtained from a comparison of the reactions of ammonia with **4** and *N*-formyloxy-*N*-methylformamide **5**. An *N*-alkyl group leads to a much larger activation energy in accordance with the experimental findings for *N*-acyloxy-*N*-alkylamides, which are resistant to attack by nucleophiles and are non-mutagenic.

Keywords: S_N2 Reactions, bionucleophiles, *N*-acyloxy-*N*-alkoxyamides

Introduction

N-acyloxy-*N*-alkoxyarylamides **1** constitute a general class of electrophilic amides that have been shown to be mutagenic.[1-5] These were first synthesised by our group in 1989 and Ames mutagenicity testing has indicated that they are direct-acting mutagens. They afford linear dose-response relationships in the TA100 strain of *Salmonella typhimurium* in the absence of metabolic activation.[5]

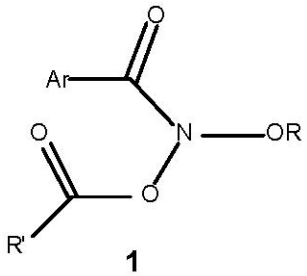

1

R=alkyl, aryloxy;
R'=CH_3, aryl

Since then, we have synthesised a wide range of substances with structural variation on all three side chains. To date, all that we have tested have exhibited mutagenicity and we have used their activity towards *Salmonella* TA100 without S9 as a measure of their relative biological activity. Recently we reported positive correlations of mutagenicity with hydrophobicity and chemical stability.[5]

Structurally, these mutagens are members of the class of so-called *anomeric amides* which have two electronegative atoms bonded to the amide nitrogen.[6-9] This results in strong pyramidalisation of the amide nitrogen to satisfy the electron demand of the heteroatoms and the nitrogen lone pair is consequently far less conjugated with the amide carbonyl than is the case in primary amides, secondary and tertiary *N*-alkylamides, or even hydroxamic esters which have only one oxy-substituent. Such amides have high carbonyl stretch frequencies (1720-1740cm^{-1}) and low amide isomerisation barriers (Figure 1(a)) and, in addition, they can support an anomeric effect at the amide nitrogen.[6-8] The lone pair on one heteroatom can interact with the σ* orbital between the amide nitrogen and the other heteroatom (Figure 1(b)).

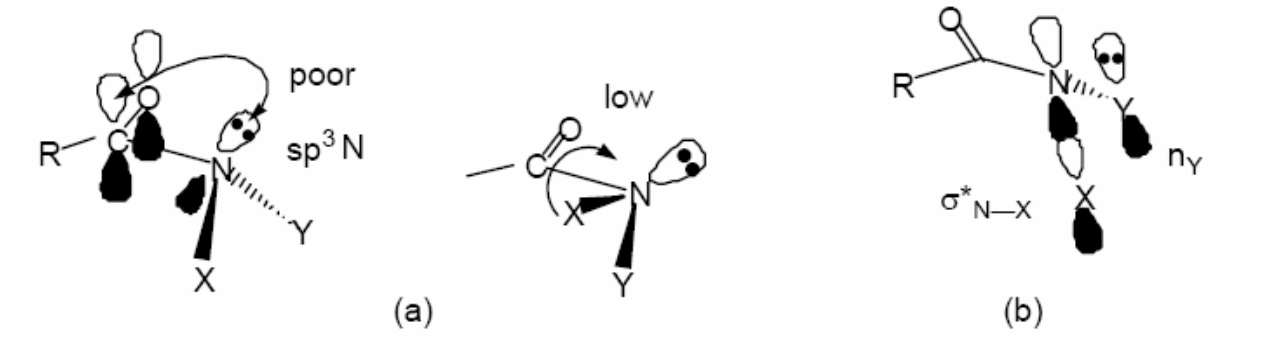

Figure 1. (a) Pyramidalisation and (b) anomeric interactions in bisheteroatom-substituted amides.

Chemical reactivity studies have highlighted two principal modes of reactivity for amides of type **1**. They undergo S_N1-type and S_N2-type reactions at the amide nitrogen and, as such, they are novel electrophilic amides. In the presence of acid, they generate *N*-acyl-*N*-alkoxynitrenium ions by the $A_{Al}1$ catalysed mechanism (Scheme 1) but react rather slowly in a neutral, aqueous organic environment.[3,4] In the presence of base[4] and organic amines[10] they have been found to react by an S_N2 process involving direct substitution of the acyloxy group at nitrogen (Scheme 2). In the case of amines, the resultant anomeric *N*-amino-*N*-alkoxyamides are unstable and undergo a novel rearrangement leading to the generation of esters and 1,1-diazenes, the so-called HERON reaction.[7,10-13] Recent results have indicated that the mutagens are also susceptible to bimolecular reactions with the cellular conjugating agent glutathione and azide.[14,15]

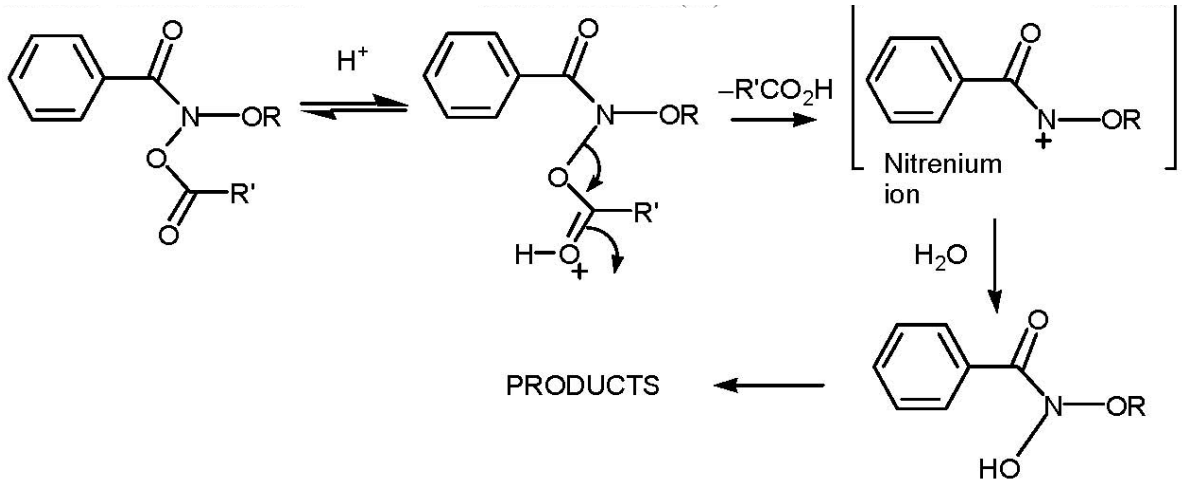

Scheme 1

Not only might *N*-acyloxy-*N*-alkoxyamides react with intracellular nucleophiles, their reactivity with DNA involves bimolecular reactions with electron-rich centres on DNA bases. N7 of guanine in the major groove as well as N3 of adenine in the minor groove are both targets of electrophiles in DNA and we have recently shown that a number of mutagens in this class react with DNA at these centres.[16]

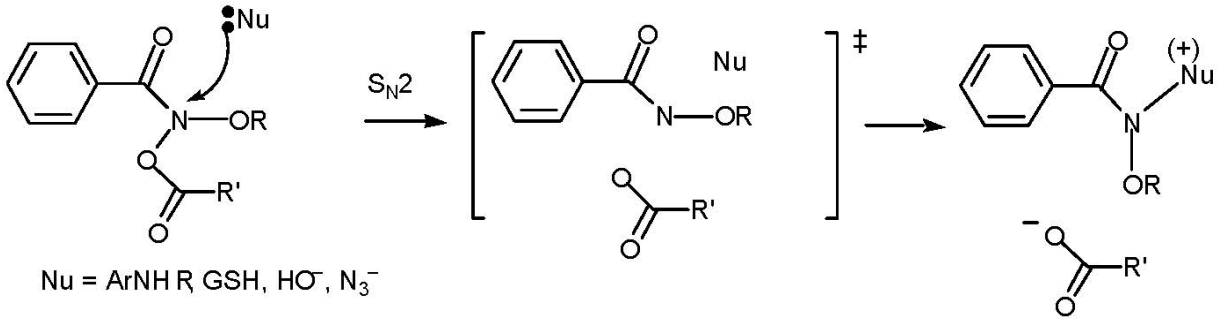

Scheme 2

S_N2 reactions at amide nitrogens is unusual and is made possible in these substances, firstly by sp3 hybridisation of the amide nitrogen; S_N2 displacement of leaving groups at sp^2 hybridised nitrogen of simple amides would be analogous to substitutions at vinyl carbons. Secondly, the *N–OCOR'* bond is anomerically weakend by the geminal alkoxy group through overlap of its p-type lone pair with the *N–OCOR'* σ*orbital.[7] Evaluation of activation energies

and entropies of activation for the reaction of a range of mutagens with *N*-methylaniline as well as the reaction of a series of substituted anilines with *N*-acetoxy-*N*-butoxybenzamide have highlighted unusual features of the transition state for bimolecular reactions with nitrogen nucleophiles (Figure 2).[10]

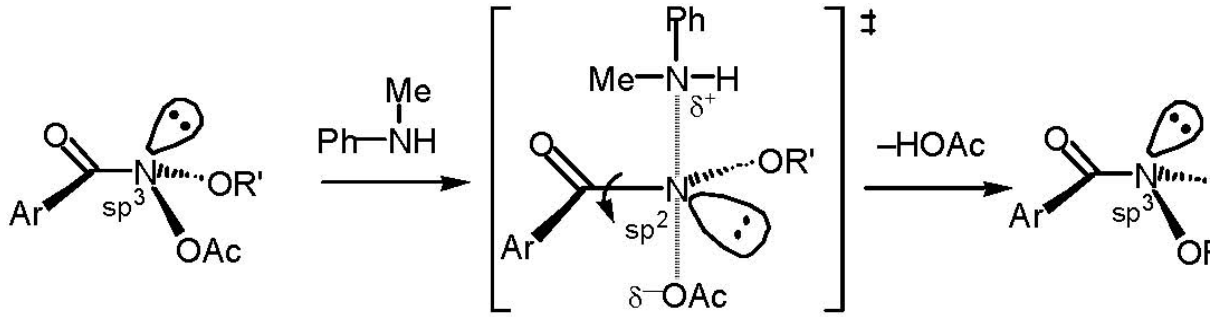

Figure 2. Reaction of *N*-methylaniline with mutagenic *N*-acetoxy-*N*-alkoxybenzamides.

The activation energies are modest and reflect not only the partial bond formation/breaking in a normal S_N2 reaction, but also the loss of lone pair conjugation in the ground state which, although less than in simple amides,[6,7] is likely to make up a significant portion of the energy barrier. In addition, while S_N2 reactions of alkyl halides by anionic displacement involving charge delocalisation exhibit entropy values in the range –40 to –20 $JK^{-1}mol^{-1}$, the entropies of activation for S_N2 reactions at the amide nitrogen are in the region of –100 $JK^{-1}mol^{-1}$ as would be expected for an associative transition state (Figure 2) in which there is increased charge separation relative to the ground state.[17] Solvation is an important contributor to the negative $\Delta S^{\ddagger}$. This effect is offset to a small extent by an increase in rotational freedom about the *N–C(O)* bond as the lone pair resides in an sp^2 hybrid orbital, rather than one with partial $2p_z$ character, and possibly relief of steric compression since there is a sharper angle at nitrogen in the ground state than in the transition state where nitrogen must be sp^2 hybridised.

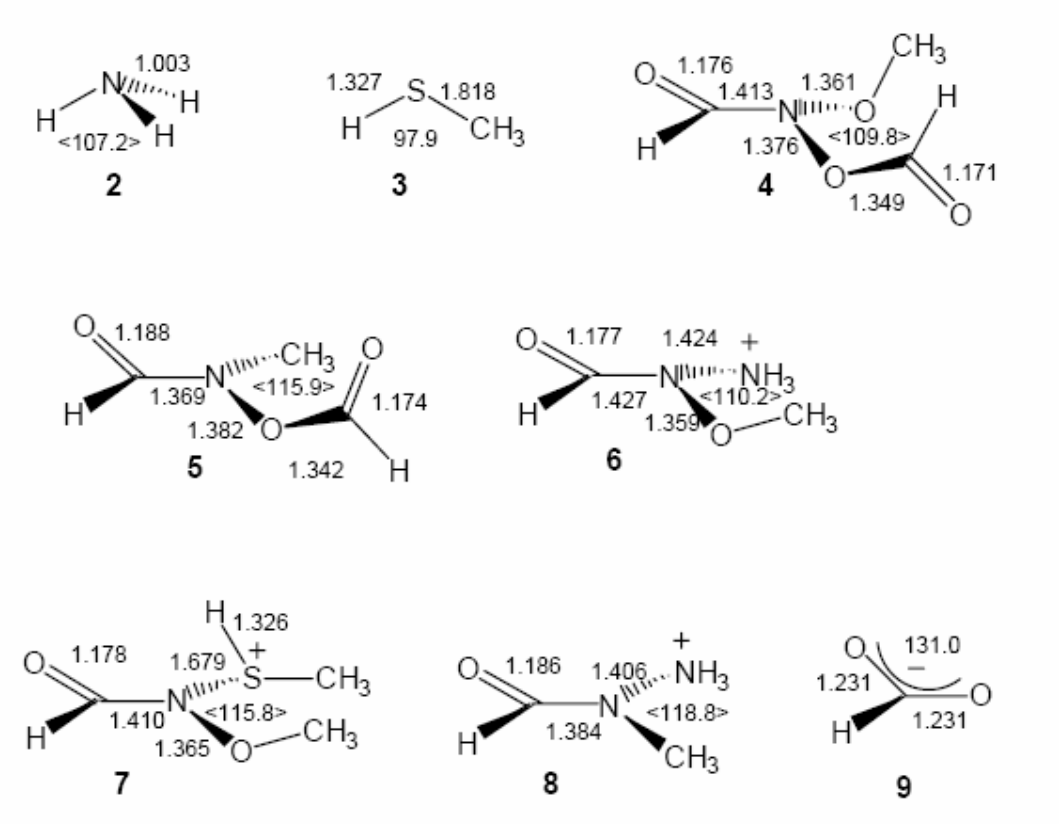

Figure 3. 6-31G*-optimised ground state structures of reactants and products. Bond lengths in angstroms, bond angles in degrees, pointed brackets denote the average of the three bond angles at nitrogen.

In this paper we report theoretical transition states for S_N2 reactions of nitrogen and sulfur nucleophiles with model mutagen *N*-formyloxy-*N*-methoxyformamide **4**. The results confirm the experimental results. Theoretical modeling of reaction with the anionic nucleophile azide will form the basis of a future publication.

Results and Discussion

6-31G*-optimised geometries for ground state reactants, ammonia **2** and the model mutagen *N*-formyloxy-*N*-methoxyformamide **4**, are given in Fig. 3 together with selected data. In accordance with previous results[6] the *N*-formyloxy-*N*-methoxyformamide conformer of lowest energy had the carbonyl and alkoxy oxygens *cis* with respect to the amide *C–N* bond. The

nitrogen is distinctly pyramidal <109.8>† resulting in a lone pair that is poorly conjugated with the amide carbonyl in keeping with the high carbonyl stretch frequencies recorded for these amides.[7] Computation of the amide rotational barrier at the density functional level of theory, which provides more reliable energies, particularly of transition states, afforded an amide *E*/*Z* isomerisation barrier in the region of 23.5 or 28.6 kJmol^{-1} depending upon the direction of rotation. This is entirely consistent with previously published theoretical data for *N*,*N*-dimethoxyformamide (29.8 kJmol^{-1}) and *N*-chloro-*N*-methoxyformamide (29.4 kJmol^{-1})[6,7] and lower than that calculated for the NNO system *N*-dimethylamino-*N*-methoxyformamide (52 kJmol^{-1}) or that determined experimentally for *N*,*N*′-diacetyl-*N*,*N*′-di(*p*-chlorobenzyloxy)hydrazine (54 kJmol^{-1}).[8,9] This low barrier accords with experimental findings for *N*-acetoxy-*N*-alkoxyamides which, unlike normal amides or hydroxamic esters, show no line broadening in their ^{1}H NMR spectra at room temperature; *N*-acetoxy-*N*-benzyloxybenzamide shows line broadening below 250K but the acetoxy methyl and benzylic methylene protons remain isochronous down to 190K indicating that barriers to isomerisation processes are below about 35 kJmol^{-1}.[7]

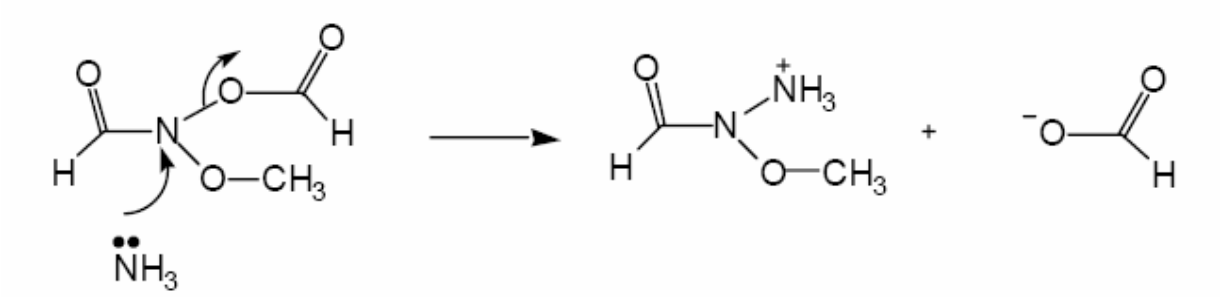

Scheme 3

The transition state for the reaction of *N*-formyloxy-*N*-methoxyformamide with ammonia (Scheme 3), was obtained at the AM1 level of theory (Figure 4(a)) and refined to the 6-31G* Hartree-Fock geometry which is illustrated in Fig. 4(b).[18] Structural and electronic properties are provided in Table 1. The transition states at the two levels of theory show distinct similarities, both having the nucleophile and leaving group displaced in the direction of the amide nitrogen lone pair. However, at the more rigorous level, the nucleophile and formyloxy leaving group are approaching linearity and the amide nitrogen lone pair, the methoxy group and the amide formyl substituent are approximately coplanar. Deviation from the classical linear transition state for S_N2 displacement at carbon is not unexpected considering the complex interplay of lone pairs on N2, O3 and O5. The methoxy group is aligned to maximise the p-type lone pair on the O5 with

the N2-O3 bond and therefore the σ^*_{NO} orbital, suggesting it plays a negative hyperconjugative role even at the transition state. The reaction is concerted, the acetoxy group departing as *N–N* bond formation occurs.[18] At the 6-31G* level of theory the amide carbonyl is close to the C4-N2-O5 plane and largely disconnected with the amide nitrogen lone pair which lies in the same plane. An estimate of the amide isomerisation barrier in the transition state could not be obtained since single point pBP calculations with different twist angles about the amide *N–CO* bond revealed that orthogonal orientations led to severe steric interactions between either the carbonyl oxygen or the formyl hydrogen and the departing formyloxy oxygen atom.

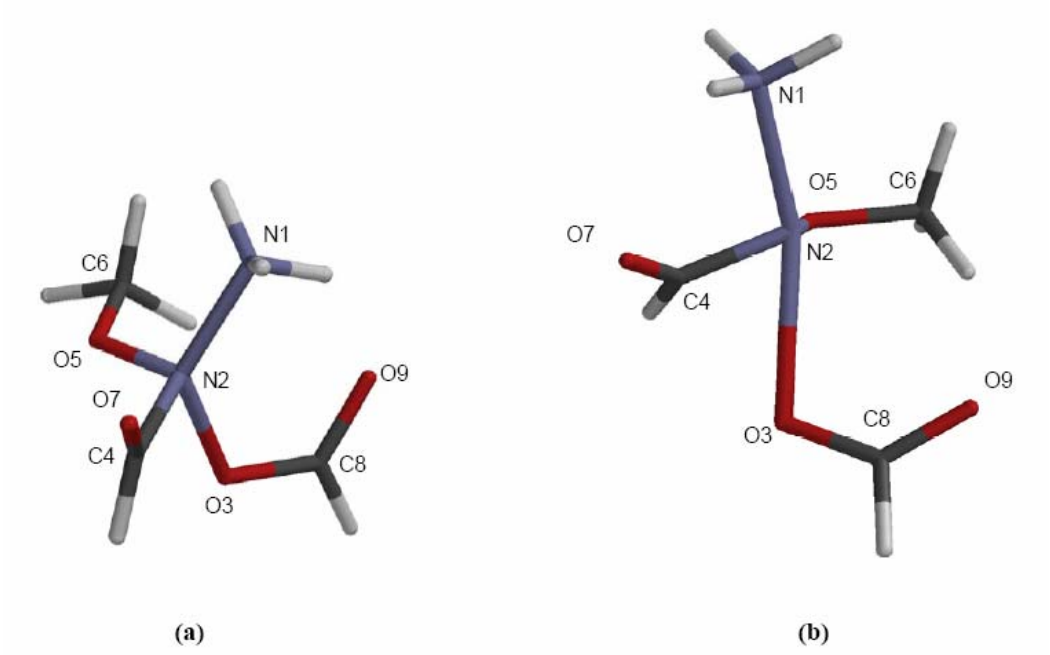

Figure 4. (a) AM1, and (b) 6-31G* optimised geometries for the transition state for the reaction of ammonia with *N*-formyloxy-*N*-methoxyformamide **4**.[18]

Table 1. Transition state geometries and properties[a]

Property	**4(a)**	**4(b)**		**5(a)**	**5(b)**		**6(a)**	**6(b)**
N1-N2	1.747	1.898	S1-N2	1.830	2.062	N1-N2	1.728	1.891
N2-O3	1.795	2.316	N2-O3	1.868	2.408	N2-O3	1.725	2.034
N2-C4	1.498	1.490	N2-C4	1.484	1.501	N2-C4	1.468	1.458
N2-O5	1.306	1.276	N2-O5	1.311	1.296	N2-C5	1.470	1.483
N1-N2-O3	132.0	155.1	S1-N2-O3	137.4	147.3	N1-N2-O3	132.9	167.8
C4-N2-O5	106.9	108.7	C4-N2-O5	110.4	109.0	C4-N2-C5	108.1	116.7
C4-N2-O3	96.3	65.1	C4-N2-O3	91.9	69.5	C4-N2-O3	98.8	77.1
C4-N2-N1	109.3	96.6	C4-N2-S1	106.7	100.3	C4-N2-N1	108.3	95.8
O5-N2-O3	99.4	98.1	O5-N2-O3	96.9	103.9	C5-N2-O3	99.0	90.5
O5-N2-N1	110.2	104.1	O5-N2-S1	110.0	108.7	C5-N2-N1	107.7	101.6
			N2-S1-C10	107.9	95.3			
O3-N2-O5-C6	-70.0	-95.1	O3-N2-O5-C6	-66.4	-80.9	O8-C4-N2-C5	-91.4	-152.8
O7-C4-N2-O5	75.1	154.9	O7-C4-N2-O5	-15.5	-14.4			
Δq (OCHO)	-0.58	-0.67	Δq (OCHO)	-0.68	-0.72	Δq (OCHO)	-0.50	-0.51
$\Delta q(NH_3)$	+0.40	+0.34	$\Delta q(CH_3SH)$	+0.25	+0.40	$\Delta q(NH_3)$	+0.38	+0.31
Δq(CHO)	-0.11	+0.03	Δq(CHO)	-0.02	+0.06	Δq(CHO)	-0.04	+0.18
Δq(N)	+0.4	+0.23	Δq(N)	+0.51	+0.25	Δq(N)	+0.22	+0.09
$\Delta q(OCH_3)$	-0.03	+0.07	$\Delta q(OCH_3)$	-0.08	+0.02	$\Delta q(CH_3)$	-0.04	-0.01
Imaginary Frequency	515	428		233	369		644	648

[a] Bondlengths in Å; bond angles and dihedral angles in degrees; group charges in electrons; frequencies in $cm^{-1.}$

AM1 and 6-31G* geometries for the transition states for reaction of methanethiol **3** with the model mutagen **4** (Scheme 4) are depicted in Figure 5(a) and Figure 5(b).[18] The sulfur and formyloxy groups have a similar disposition relative to transition states 4(a) and 4(b) although both methods predict a more advanced transition state than is the case for attack of ammonia; both computational methods predict the N2–O3 bond to be significantly longer in each of the thiomethyl transition states. At the 6-31G* level, the thiol group clearly reacts through the p-type lone pair on the sulfur atom as evidenced by the nearly orthogonal arrangement of N2-S1-C10. Once again the p-type lone pair on O5 is largely collinear with the N2–O3 σ* orbital and the amide carbonyl is nearly in the C4-N2-O5 plane.

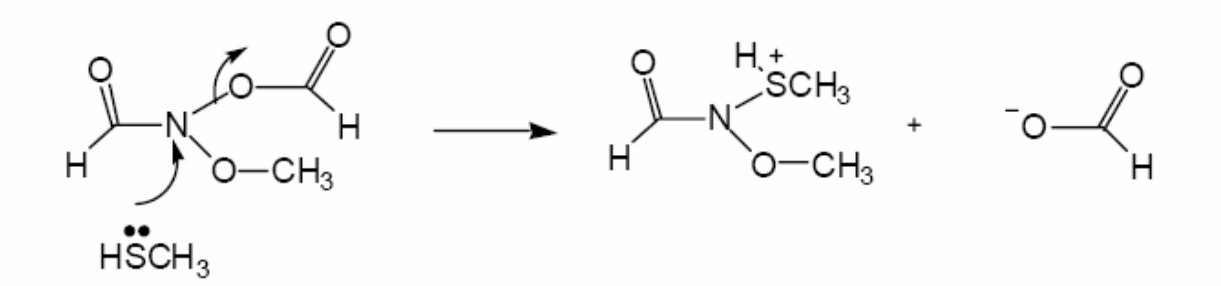

Scheme 4

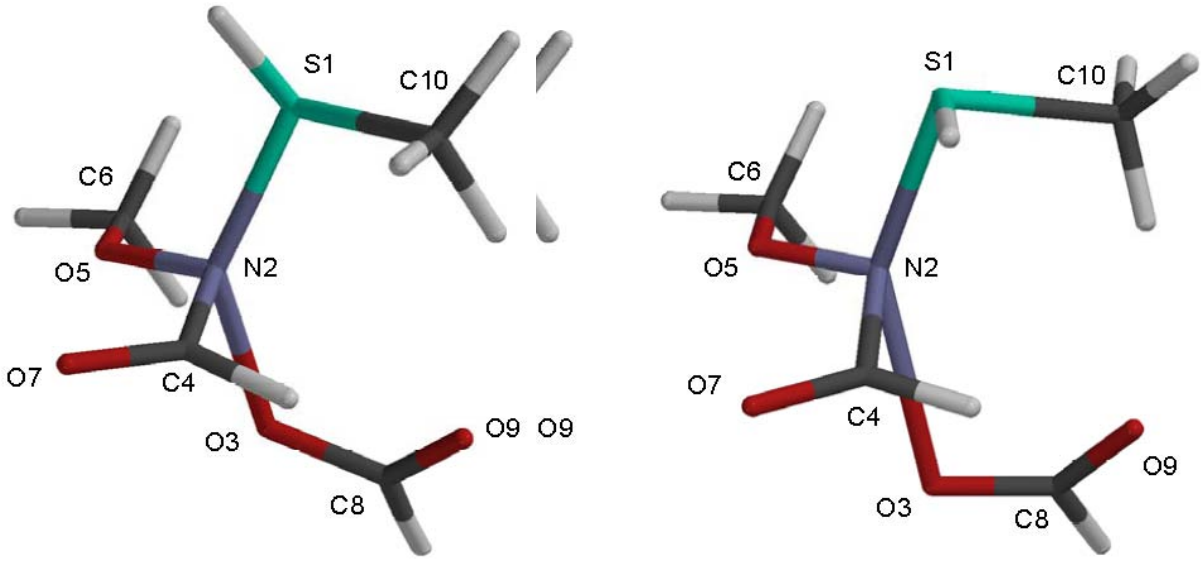

(a) **(b)**

Figure 5. (a) AM1, and (b) 6-31G* optimised geometries for the transition state for the reaction of methanethiol with *N*-formyloxy-*N*-methoxyformamide **4**.[18]

Analysis of the electrostatic charges in the ground states of the reactants and their respective transition states supports the experimental solvation effect described in the introduction. Table 1 gives the changes in total charge on the nucleophile and the formyloxy leaving group in each of the transition states depicted in Figure 4 and Figure 5. The greater build-up of negative charge in the formyloxy group compared to positive charge accrual on the nucleophiles is indicative of a non-synchronous process and of partial nitrenium ion character in the transition state. Detailed analysis of the charges on each fragment along the reaction coordinate is illuminating. The relative energy, solvation energy and corresponding changes in charge on the ammonia, formate, methoxyl, formyl and amide nitrogen fragments along the virtual vibration18 representing the reaction coordinate for the reaction of ammonia **3** with *N*-formyloxy-*N*-methoxyformamide **4** are illustrated in Figure 6.

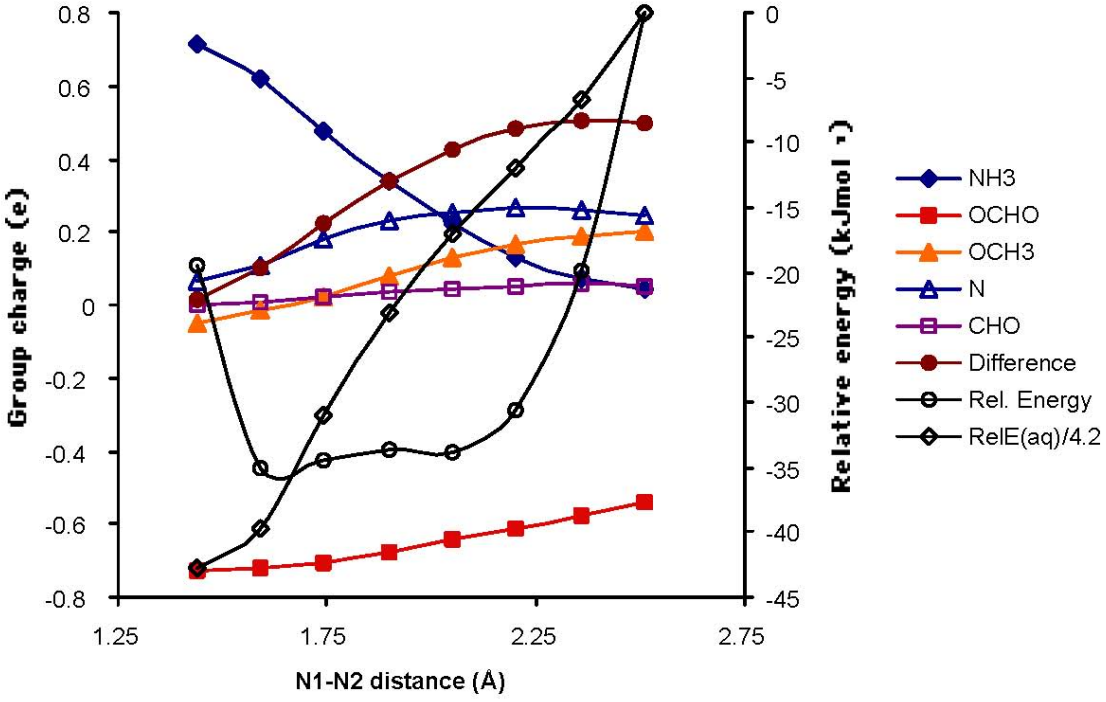

Figure 6. 6-31G* relative energies and group charges along the imaginary vibration of transition state 4(b)[18]

Clearly, even at the N1-N2 bond distance of 2.5Å, where the charge on ammonia is only +0.04 and the geometry at nitrogen is virtually unchanged and tetrahedral, the formate has well developed anionic character (-0.54). The "difference" plot depicts the total positive charge on the central fragments [-Δq(OCHO)-Δq(NH_3)]. Initially, the difference in charge (+0.54) resides mainly on the amide nitrogen and the methoxyl group and represents partial alkoxynitrenium ion character. This is only partially transferred to the ammonia nitrogen at the transition state (N1-N2 = 2.06Å) and the bulk of the difference in charge is computed to reside on the amide nitrogen. This is in accord with experimental data which indicated a smaller Hammett reaction constant for the reaction of a series of substituted anilines with *N*-acetoxy-*N*-butoxybenzamide ($\rho = -0.9$[10]) when compared to aniline reactions at alkyl or acyl centres ($\rho = -2.0$ to -3.0)[19] indicating that positive charge, formed as a result of loss of acetate, is not fully transferred to the aniline, residing instead on the alkoxyamide structure. The "Rel E(aq)" curve gives scaled relative solvation energies along this virtual vibration as estimated for water by the SM5.4 method and reflects the increasing charge separation as ammonia reacts at the amide nitrogen.

Table 2. pBP/DN*//6-31G* energies of reactants, transition states and products[a]

Substrate	E/Hartree	Eaq/Hartree
NH_3 **2**	-56.57419	-56.58491
CH_3SH **3**	-438.77211	-438.77458
$CHON(OCHO)OCH_3$ **4**	-473.05454	-473.05540
$CHON(OCHO)CH_3$ **5**	-397.86257	-397.86980
$[CHON(NH_3)OCH_3]+$ **6**	-340.14775	-282.45788
$[CHON(SHCH_3)OCH_3]+$ **7**	-722.34182	-217.89337
$[CHON(NH_3)CH_3]+$ **8**	-264.95612	-293.17050
HCO_2^- **9**	-189.29648	-306.59737
T.s. Fig. 4(b)	-529.60117	-529.64167
T.s Fig. 5(b)	-911.79233	-911.82333
T.s. Fig. 7(b)	-454.38013	-454.41220

[a] Lowest energy conformers; ZPE not included.

Table 3. pBP/DN*//6-31G* *E*A's and Reaction Energies[a]

Reaction	*E*A/kJmol^{-1}	Reaction Energies /kJmol^{-1}
NH_3 + CHON(OCHO)OCH_3 **4**	72.37 (-3.58)	484.34 (-74.34)
CH_3SH + CHON(OCHO)OCH_3 **4**	90.08 (17.43)	494.43 (-21.35)
NH_3+ CHON(OCHO)CH_3 **5**	148.65 (111.68)	483.42 (-69.15)

[a] Values in parenthesis take into account aqueous solvation of reactants, transition states and products.

While experimental geometries are reliably computed at the Hartree-Fock level with the large 6-31G* basis set, *E*A's and Reaction Energies are obtained more accurately from correlated methods or density functional theory. For the reactions between *N*-formyloxy-*N*-methoxyformamide **4** and ammonia **2** or methanethiol **3**, E_A's and Reaction Energies were therefore estimated at the pBP/DN* level of theory from single point calculations on the 6-31G* optimised geometries for the ground state reactants, products and transition states 4(b) and 5(b) (Tables 2 and 3). The gas-phase E_A of 72.6 kJmol^{-1} for the reaction with ammonia compares reasonably well with experimental values for substitution by *N*-methylaniline in methanol which fall in the range of 40-65 kJmol^{-1}.[10] The methanethiol reaction is computed to have a slightly higher activation energy of 90.4 kJmol^{-1} and has not yet been determined experimentally. Table 2 also provides pBP single point energies adjusted for the effect of solvation in water as estimated from the SM5.4 semiempirical solvation energies and estimated E_A's and Reaction Energies in aqueous solution are presented in parentheses in Table 3. In accordance with the increased charge separation in the transition states, polar solvents should radically decreases these barriers and the Reaction Energies, which in the gas phase are strongly endothermic, become exothermic.

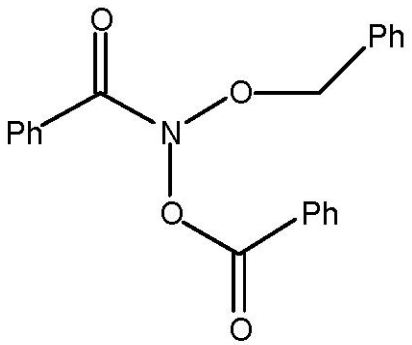

10

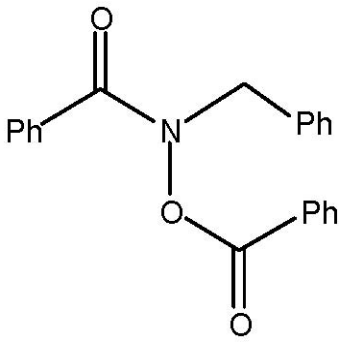

11

The role of the alkoxy oxygen in destabilising the acyloxy oxygen–nitrogen bond in these reactions is evident from the apparent lack of nucleophilic reactivity and biological activity of *N*-acyloxy-*N*-alkylamides. Whereas *N*-benzoyloxy-*N*-benzyloxybenzamide **10**, like all other members of this class, is significantly mutagenic,[5] the analogous *N*-benzoyloxy-*N*-benzylbenzamide **11** is non-mutagenic.[20] Recent results in these laboratories have also shown that **11** also fails to react directly with DNA whereas **10** damages N7 of guanine and N3 of adenine in the major and the minor grooves of DNA respectively.16 In addition, **11** fails to react with azide.[15] The anomeric weakening by the alkoxy oxygen is therefore an important factor in the reactivity of *N*-acyloxy-*N*-alkoxyamides. Calculations on the transition state and ground-state reactants for the reaction of ammonia with model *N*-formyloxy-*N*-methylformamide **5** (Scheme 5), confirm this.

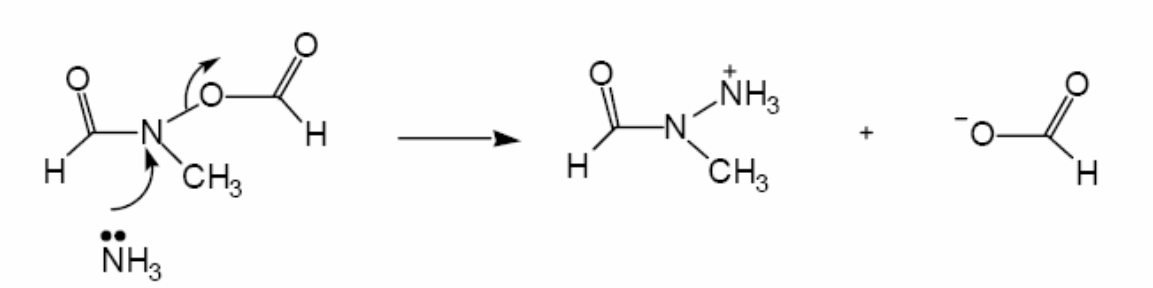

Scheme 5

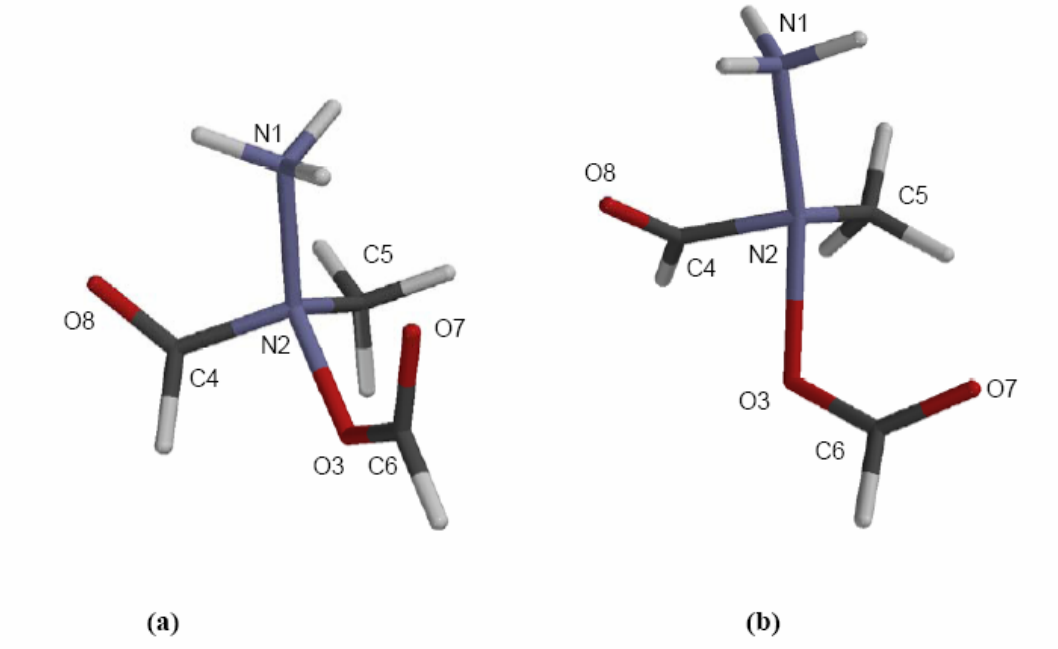

Figure 7. (a) AM1, and (b) 6-31G* optimised geometries for the transition state for the reaction of ammonia with *N*-formyloxy-*N*-methylformamide **5**.[18]

The 6-31G* derived lowest energy conformer of *N*-formyloxy-*N*-methylformamide **5** is illustrated in Figure 3. The structure shown with oxygens *anti* is lower in energy than the *syn* isomer by 6.7 kJmol^{-1}. The nitrogen is moderately pyramidal <115.9> and the lowest energy transition state for isomerisation between these two diastereomeric forms is 43.9 kJmol^{-1}, slightly lower than the computed barriers for the closely related *N*-methoxyformamide which had a barrier to isomerisation of 64 kJmol^{-1}(B3LYP/6-31G*[6]). Figure 7 illustrates the AM1 and 6-31G* optimised geometries for the transition states and selected transition state properties are given in Table 1. There are a number of important differences between these optimised transition structures and those for the methoxylated substrate, 4(a) and 4(b). The N2–O3 bond is significantly shorter in this transition state and the combined charge on the formate leaving group is not as negative (-0.51 *versus* -0.67). This suggests a stronger bond between the amide nitrogen and the formyloxy group with less charge separation and solvation of the transition state would be less important. A non-synchronous transition state is again evident18 but, whereas in transition state 4(b) there is significant nitrenium ion character, there is much less positive charge on the amide nitrogen in transition state 7(b). The pBP/DN*//6-31G* energies of reactants and products and the E_A and Reaction Energy for this reaction are presented in Tables 2 and 3. Table 3 indicates that the gas-phase E_A for this reaction is nearly 80 kJmol^{-1} higher with an *N*-methyl as opposed to an *N*-methoxy group and is in accord with a stronger *N–OCHO* bond. In addition, the effect of an aqueous environment is computed to be smaller, which is consistent with less charge separation in the transition state. Clearly S_N2 reactivity would not be expected to occur as readily with *N*-alkyl-*N*-acyloxyamides and this difference mirrors the known S_N2 reaction rate enhancements at carbon centres flanked by heteroatoms or pi systems. We have previously described the strong stabilisation of nitrenium ions by lone pairs on an adjacent alkoxy oxygen atom;21 alkoxynitrenium ions have a pi-bond order of approximately 0.9. As well as lowering its energy, this stabilisation moves the S_N2 saddle point vertical to the S_N2 reaction axis in the direction of the nitrenium ion corner resulting in incipient nitrenium ion character in the transition state structure (Figure 8).[22]

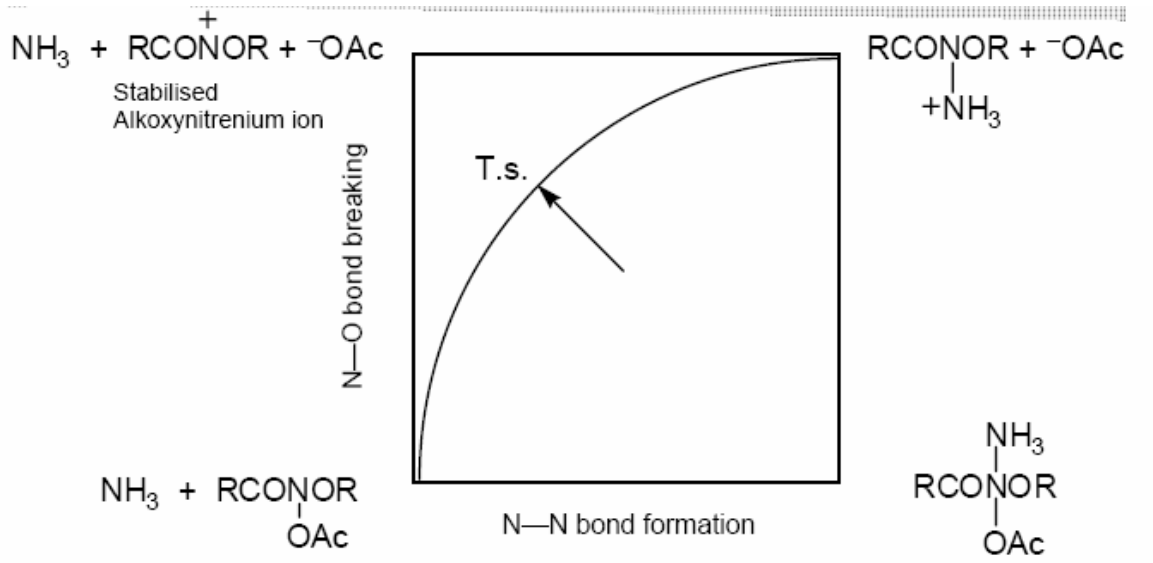

Figure 8. Two-dimensional reaction coordinate for the reaction of ammonia with an *N*-acetoxy-*N*-alkoxyamide**.**

Finally, an analysis of the structures and energies of product ammonium and sulfonium ions **6**, **7** and **8** indicates a strong preference in all three cases for a conformation that has the formamide carbonyl *cis* to the positively charged nitrogen or sulfur atom. The alternative conformations were computed to be 36, 45 and 35 kJmol^{-1} higher in energy respectively. An attractive interaction between the positive centre and the p-type lone pair on the carbonyl oxygen would account for this. Interestingly, the presence of a strongly electron-withdrawing ammonium ion at nitrogen is, by itself, insufficient to cause significant pyramidalisation at the formamide nitrogen; the amide nitrogen of ammonium ion **8** is nearly planar (sp^2, <119>) while that of the methoxylated analogue **6** is strongly pyramidal (<110>). The additional electronegativity of the alkoxy oxygen atom in 6 is necessary to cause this alteration in geometry. A comparison of **6** or **4** with **5** is a further illustration of this pyramidalisation effect. The average angle at nitrogen in **5**, <116>, is significantly larger than that in either **6** (<110>) or **4** (<110>).

Experimental Section

General Procedures. All ground state structures were fully optimised at the AM1 followed by the HF/6-31G* levels using procedures standard to the Spartan 5 and MacSpartan Pro.[23, 24] Ground state structures were verified as having all-positive eigenvectors while transition states were shown by vibrational analysis to have one negative eigenvalue corresponding to the

reaction coordinate. Best estimates of energies of all structures were obtained from density functional theory at the pBP/DN* level[25,26] using 6-31G*-optimised geometries of ground state and transition state structures. Solvation energies were computed at the semiempirical level by the SM5.4 method of Chambers *et al.*[27] The average of all three angles at amide nitrogens was used as a measure of pyramidality; planar sp^2 and tetrahedral sp^3 hybridised nitrogens represented by the limits of <120> and <109.5> respectively**.**

Acknowledgements

The author is grateful to the Australian Research Council for financial support administered through the University of New England University Research Grants Scheme.

References and Notes

1. Gerdes, R. G.; Glover, S. A.; Ten Have, J. F.; Rowbottom, C. A. *Tetrahedron Lett.* **1989**, *30*, 2649.
2. Campbell, J. J.; Glover, S. A.; Hammond, G. P.; Rowbottom, C. A. *J. Chem. Soc. Perkin Trans. 2* **1991**, 2067.
3. Bonin, A. M.; Glover, S. A.; Hammond, G. P. *J. Chem. Soc., Perkin Trans. 2* **1994**, 1173.
4. Bonin, A. M.; Glover, S. A.; Hammond, G. P. *J.Org. Chem.* **1998**, *63*, 9684.
5. Bonin, A. M.; Banks, T. M.; Campbell, J. J.; Glover, S. A.; Hammond, G. A.; Prakash, A. S.; Rowbottom, C. A. *Mutat. Res.* **2001**, *494*, 115.
6. Glover, S. A.; Rauk, A. *J.Org.Chem.* **1996**, *61*, 2337.
7. Glover, S. A. *Tetrahedron* **1998**, *54*, 7229. Tetrahedron Report 455.
8. Glover, S.; Rauk, A. *J.Org. Chem.* **1999**, *64*, 2340.
9. Glover, S. A.; Mo, G.; Rauk, A.; Tucker, D.; Turner, P. *J. Chem. Soc. Perkin Trans. 2* **1999**, 2053.
10. Campbell, J. J.; Glover, S. A. *J. Chem. Res. (S)* **1999**, *8*, 474. *J. Chem. Res. (M)*, 2075.
11. Buccigross, J. M.; Glover, S. A. *J. Chem. Soc., Perkin Trans. 2* **1995**, 595.
12. Buccigross, J. M.; Glover, S. A.; Hammond, G. P. *Aust. J. Chem.* **1995**, *48.*, 353.
13. Glover, S. A.; Mo, G.; Rauk, A. *Tetrahedron* **1999**, *55*, 3413.
14. Glover, S. A.; Tucker, D. J. Unpublished results.
15. Mo, G. Ph.D. Thesis, University of New England, 1999.
16. Banks, T. M.; Glover, S. A.; Prakash, A. S. Recent unpublished results.

17. Isaacs, N. S. *Phys.Org. Chem.,* 2nd Edn; Longman Scientific and Technical: New York, 1995.
18. Hyperactive versions of transition states depicted in Fig. 4(b), Fig. 5(b) and Fig. 7(b) as well as the virtual vibrations corresponding to each transition state may be viewed at <http://www-personal.une.edu.au/~sglover/>.
19. Jaffé, H. H. *Chem. Rev.* **1953**, *53*, 191.
20. Banks, T. M.; Bonin, A.; Glover.S.A. . Recent unpublished results.
21. Glover, S. A.; Scott, A. P. *Tetrahedron* **1989**, *45*, 1763.
22. Harris, J. M.; Shafer, S. G.; Moffatt, J. R.; Becker, A. R. *J. Am. Chem. Soc.* **1979**, *101*, 3295.
23. Spartan Version 5; Wavefunction, Inc.; 18401 Van Karman, Suite 370, Irvine, California, 92612.
24. MacSpartan *Pro* Version 1; Wavefunction, Inc.; 18401 Van Karman, Suite 370, Irvine, California, 92612.
25. Becke, A. D. *Phys. Rev. A* **1988**, *38*, 3098.
26. Perdew, J. P. *Phys. Rev. B* **1986**, *33*, 8822.
27. Chambers, C. C.; Hawkins, G. D.; Cramer, C. J.; Truhlar, D. G. *J. Phys. Chem.* **1996**, *100*, 16385.